Electronic structure and optical properties of $ZnSiO_3$ and Zn_2SiO_4

S. Zh. Karazhanov, P. Ravindran, H. Fjellvåg, and B. G. Svensson

Citation: Journal of Applied Physics **106**, 123701 (2009); doi: 10.1063/1.3268445
View online: http://dx.doi.org/10.1063/1.3268445
View Table of Contents: http://aip.scitation.org/toc/jap/106/12
Published by the American Institute of Physics

Articles you may be interested in

Formation mechanism of $ZnSiO_3$ nanoparticles embedded in an amorphous interfacial layer between a ZnO thin film and an n–Si (001) substrate due to thermal treatment
Journal of Applied Physics **103**, 083520 (2008); 10.1063/1.2902477

Preparation and characterization of ZnO particles embedded in SiO_2 matrix by reactive magnetron sputtering
Journal of Applied Physics **97**, 103509 (2005); 10.1063/1.1897493

Luminescence thermometry with Zn_2SiO_4:Mn^{2+} powder
Applied Physics Letters **103**, 141912 (2013); 10.1063/1.4824208

Transformation mechanisms from metallic Zn nanocrystals to insulating $ZnSiO_3$ nanocrystals in a SiO_2 matrix due to thermal treatment
Applied Physics Letters **93**, 221910 (2008); 10.1063/1.3040320

Mechanisms behind green photoluminescence in ZnO phosphor powders
Journal of Applied Physics **79**, 7983 (1998); 10.1063/1.362349

AIP | Journal of Applied Physics
Save your money for your research.
It's now FREE to publish with us -
no page, color or publication charges apply.
Publish your research in the
Journal of Applied Physics
to claim your place in applied
physics history.

Electronic structure and optical properties of $ZnSiO_3$ and Zn_2SiO_4

S. Zh. Karazhanov,[1,2,a)] P. Ravindran,[1] H. Fjellvåg,[1] and B. G. Svensson[3]
[1]Department of Chemistry, Centre for Material Science and Nanotechnology, University of Oslo, P.O. Box 1033 Blinden, N-0315 Oslo, Norway
[2]Institute for Energy Technology, P.O. Box 40, NO-2027 Kjeller, Norway
[3]Department of Physics, University of Oslo, P.O. Box 1048 Blindern, N-0316 Oslo, Norway

(Received 8 September 2009; accepted 29 October 2009; published online 16 December 2009)

The electronic structure and optical properties of orthorhombic, monoclinic, and rhombohedral (corundum type) modifications of $ZnSiO_3$, and of rhombohedral, tetragonal, and cubic (spinel type) modifications of Zn_2SiO_4 have been studied using *ab initio* density functional theory calculations. The calculated fundamental band gaps for the different polymorphs and compounds are in the range 2.22–4.18 eV. The lowest conduction band is well dispersive similar to that found for transparent conducting oxides such as ZnO. This band is mainly contributed by Zn 4*s* electrons. The carrier effective masses were calculated and compared with those for ZnO. The topmost valence band is much less dispersive and contributed by O 2*p* and Zn 3*d* electrons. From the analysis of charge density, charges residing in each site, and electron localization function, it is found that ionic bonding is mainly ruling in these compounds. The calculated optical dielectric tensors show that the optical properties of $ZnSiO_3$ and Zn_2SiO_4 are almost isotropic in the visible part of the solar spectra and depend negligibly on the crystal structure. Within the 0–4 eV photon energy range, the calculated magnitude of the absorption coefficient, reflectivity, refractive index, and extinction coefficient are smaller than 10^3 cm^{-1}, 0.15, 2.2, and 0.3, respectively, for all the $ZnSiO_3$ and Zn_2SiO_4 phases considered in this work. This suggests that zinc silicates can be used as antireflection coatings. © *2009 American Institute of Physics*. [doi:10.1063/1.3268445]

I. INTRODUCTION

$ZnSiO_3$ shows useful properties such as excellent adhesion to steel surfaces, high heat resistance, high hardness, abrasion resistance, inertness to crude and refined oils, greases, and solvents, resistance to radiation (including nuclear radiation), and weather resistance. These silicates are predominantly used for buildings, offshore constructions, and bridges. They can be used as abrasion-resistant coating with controlled electrical conductivity. $ZnSiO_3$ is very inert and, with exception of exposure to strong acids and alkalides, do not degrade in most industrial and marine environments.[1] Nanodispersed $ZnSiO_3$ codeposited on nickel-phosphorus alloys are corrosion[2] as well as high-temperature oxidation resistant. Recently, a new crystalline phase of $ZnSiO_3$ is reported,[3] formed upon irradiation of nanocomposite $ZnO-SiO_2$ films with ultraviolet light. This crystalline phase is formed within the amorphous media by a photoinduced reaction. The monoclinic $ZnSiO_3$ nanocrystals have been formed as a result of rapid thermal annealing of SiO_2 with metallic Zn nanocrystals.[4] Also by the transmission electron microscopy (TEM) $ZnSiO_3$ nanoparticles have been found in between the ZnO thin film and the Si substrate.[5] Moreover, from x-ray diffraction (XRD), TEM, and selected-area electron diffraction studies, orthorhombic $ZnSiO_3$ is found at the interface of the ZnO/Si heterostructure after annealing at 900 °C resulting from the interdiffusion between ZnO and Si.[6]

Zn_2SiO_4 is known under the mineralogical name willemite and belongs to the family of orthosilicates.[3] It has numerous technological applications such as phosphor host, crystalline phase in glass ceramics, electrical insulators, glazes, and pigments (see, e.g., Ref. 7). Because of its unique luminescent properties, wide energy band gap (5.5 eV), and excellent chemical stability, Zn_2SiO_4 is candidate for flat panel displays,[8–13] x-ray or nuclear medical image receptors, x ray to light converters coupled to optical detectors,[14] etc. Zn_2SiO_4 forms readily at the interface of ZnO/Si heterostructures.[15–17] Such ZnO deposited on silicate glass is used as a transparent conducting oxide (TCO) buffer in photovoltaic solar cells.[18] Zn_2SiO_4 has a large band offset (Fig. 1),[17] which can be one of the reasons for low 8.5% efficiency of crystalline Si–ZnO solar cells.[18] Using secondary ion mass spectroscopy, a vast interdiffusion was confirmed at the interface between ZnO film and Si substrate.[15] By means of cathodoluminescence and glancing-angle XRD, the tetrago-

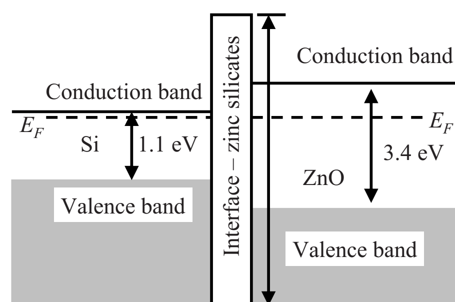

FIG. 1. Band diagram for the Si–ZnO heterojunction with interface layer of zinc silicates located in between Si and ZnO.

a)Author to whom correspondence should be addressed. Electronic mail: smagul.karazhanov@ife.no.

 © 2009 American Institute of Physics

nal modification of Zn_2SiO_4 was proved to be present. Moreover, XRD measurements have shown the existence of an earlier unknown rhombohedral modification of Zn_2SiO_4 at the boundary between ZnO particles and SiO_2 matrix.[19]

Some information on electronic structure studies of $ZnSiO_3$, Zn_2SiO_4, and similar compounds are already available. For example, Zn_2SiO_4 has been studied by the self-consistent-field multiple-scattering $X\alpha$ cluster method,[8,20] and hexagonal and tetragonal phases of Zn_2SiO_4 (Ref. 21) by the Vienna *ab initio* simulation package (VASP).[22] Fayalites M_2SiO_4 (M=Fe and Co) have been investigated[23] by the generalized-gradient approximation with the multiorbital mean-field Hubbard potential (U). The related compounds Zn_2SnO_4, Cd_2SnO_4, and In_2CdO_4 have been examined[24] by VASP. Possibility of phase transitions between structural polymorphs of $ZnSiO_3$ and Zn_2SiO_4 have been reported[25] by density functional theory (DFT) calculations using the VASP package. However, to our knowledge, there is no systematic study on the electronic structure and optical properties of the different polymorphs of $ZnSiO_3$ and Zn_2SiO_4.

Knowledge on the electronic structure and optical property for zinc silicates are of interest for semiconductor electronics. Since the electronic structure of zinc silicates are quite different from those of ZnO, Si, and SiO_2, any formation of zinc silicates at the interfaces can strongly influence optical and electrical properties of ZnO–Si and ZnO–SiO_2 based optoelectronic devices. The above mentioned experimental results about existence of different polymorphs of the zinc silicates, possibility of their formation at the interface between ZnO–Si and ZnO–SiO_2, create the necessity to study dependence of the electronic structure, electrical, and optical properties of the silicates on crystal structure and crystallographic directions. The other interesting point is dopability of the silicates by shallow level impurities and H, which would allow one to classify the silicates as semiconductors or insulators. Another interesting point to be explored is the suggestion regarding usage of Zn_2SiO_4 and $ZnSiO_3$ as passivation layers and studies of band alignment between the zinc silicates with other semiconductors. We hope that these points will motivate studies on these materials in the future. The aim of the present work is to study the electronic structure and optical properties of various polymorphs such as monoclinic (m), orthorhombic (o), and rhombohedral (r) $ZnSiO_3$ as well as tetragonal (t), cubic (c), and r-Zn_2SiO_4.

II. COMPUTATIONAL DETAILS

Information on the crystal structures of the different crystallographic modifications of $ZnSiO_3$ and Zn_2SiO_4 and corresponding positional and lattice parameters used in the present calculations are reported elsewhere (Ref. 25). For the studies of electronic structures and optical spectra, the VASP package[22] was used. The exchange and correlation energies were described by the Perdew–Zunger parametrization[26] of the quantum Monte Carlo results of Ceperley–Alder.[27] The interaction between electrons and atomic cores was described by means of non-norm-conserving pseudopotentials generated in accordance with the projector-augmented wave method.[28,29] Orthonormalized all-electron-like wave functions have been constructed for the Zn $3d$ and Zn $4s$, Si $3s$ and Si $3p$, as well as O $2s$ and O $2p$ valence electrons. Spin-orbit coupling has not been included in the present calculations.

The diagonal elements of the effective mass tensor for the conduction band (CB) electrons are calculated by

$$\frac{1}{m_c(k)} = \left. \frac{1}{\hbar^2}\frac{\partial^2 E(k)}{\partial^2 k} \right|_{k=k_0} \quad (1)$$

in different directions in k space from the Γ point toward the other high-symmetry points in the Brillouin zone. We use this to give an indication for the carrier mobility, since the CB minimum of the band dispersions of all the compounds considered are located at the Γ point of the Brillouin zone. The band edge energies $E(k)$ have been extracted from DFT calculations and ninth order polynomial fitting has been performed. From the fitted polynomial, the second order derivative was calculated, which was used in the effective mass calculations in Eq. (1).

The imaginary part of the optical dielectric function $\varepsilon_2(\omega)$ has been derived from DFT results by summing all allowed direct transitions from occupied to unoccupied states. From that the real part of the dielectric function $\varepsilon_1(\omega)$ is calculated using the Kramer–Kronig transformation. The knowledge of both the real and imaginary parts of the dielectric tensor allows one to calculate other important linear optical properties. In this paper, we present and analyze the reflectivity $R(\omega)$, the absorption coefficient $\alpha(\omega)$, the refractive index $n(\omega)$, and the extinction coefficient $k(\omega)$. More details about the optical calculations are discussed in Refs. 30 and 31.

III. RESULTS AND DISCUSSION

A. Band structure

The electronic band structures are studied for the optimized crystal structures of various polymorphs of $ZnSiO_3$ and Zn_2SiO_4 (Fig. 2). The corresponding band gaps (E_g) were determined for both of the compounds (Table I). In the present computations, no band gap correction schemes have been applied. Hence the calculated fundamental band gaps are underestimated because of the well-known deficiency of DFT. The experimental E_g value for Zn_2SiO_4-r is in the range from 5.50 to 6.26 eV. The band gap of 4.36 eV estimated from the band diagram for Si–ZnO heterojunction based on the x-ray photoelectron spectroscopy studies[17] corresponds probably to Zn_2SiO_4-t. The experimental band gap value for $ZnSiO_3$ and other polymorphs of Zn_2SiO_4 are not yet available. The band gaps calculated by DFT within local density approximation are likely to be about ~30%–50% smaller than actual experimental values. The real band gaps for these zinc silicates are expected to be ~5.0 eV. These are hence classified as wide band gap solids.

In order to understand whether the considered compounds remain transparent in the visible spectra even after heavy doping by shallow donors, the difference in the energies between the CB minimum and the second nearest CB E_g^s has been calculated (Table I), also known as the second band

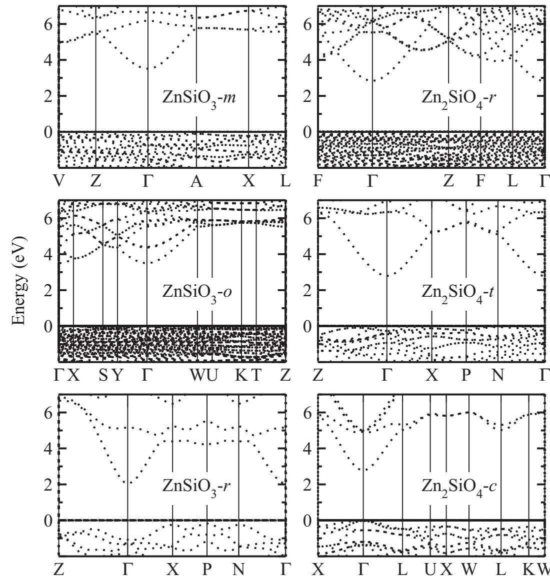

FIG. 2. Band structure for polymorphs of $ZnSiO_3$ and Zn_2SiO_4 in the high symmetry directions of the Brillouin zone. The Fermi level is set to zero.

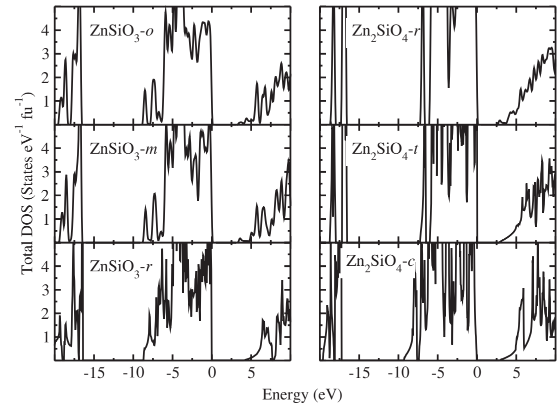

FIG. 3. Total DOS for $ZnSiO_3$ and Zn_2SiO_4 polymorphs. The Fermi level is set to zero.

gap.[24] The analysis shows that the value of E_g^s for $ZnSiO_3$-*r* is ~2.8 eV. Consequently, if $ZnSiO_3$-*r* can possess *n*-type metalliclike electrical conductivity, it can be considered as TCO. For the other $ZnSiO_3$ and Zn_2SiO_4 polymorphs, the calculated E_g^s values are smaller than 2.5 eV. The value of E_g^s depends on the crystal structure and the particular chemical composition.

The bands around the valence band (VB) maximum are very close to each other for the various $ZnSiO_3$ and Zn_2SiO_4 polymorphs and consequently, it is hard for the eye to analyze the dispersion as well as the character of the topmost VB. In Fig. 2 the band structures are therefore plotted in the vicinity of the fundamental band gap. This allows us to classify these semiconductors as either direct or indirect band gap materials. In Fig. 2 the dispersion of the band around the VB maximum is clearly seen for $ZnSiO_3$-*r*, Zn_2SiO_4-*t*, and Zn_2SiO_4-*c*. For the other $ZnSiO_3$ and Zn_2SiO_4 polymorphs, the plotting of VB is done for a very small energy range, i.e., −0.4 to 0.0 eV. For all the considered polymorphs of $ZnSiO_3$ and Zn_2SiO_4, the CB minimum is located at the Γ point (see Fig. 2). The VB maximum for $ZnSiO_3$-*o*, and Zn_2SiO_4-*r*, Zn_2SiO_4-*t*, and Zn_2SiO_4-*c* are located at the Γ point and hence they can be classified as direct band gap semiconductors, see Table I. However, the VB maxima for both $ZnSiO_3$-*m* and Zn_2SiO_4-*r* are located aside the Γ point. So, these two polymorphs have an indirect band gap.

TABLE I. Calculated fundamental band gap E_g, second gap E_g^s, and experimental gap E_g^{exp} (in eV) for polymorphs of $ZnSiO_3$ and Zn_2SiO_4.

Compound	E_g		E_g^s	E_g^{exp}
$ZnSiO_3$-*o*	3.50	Direct	0.86	
$ZnSiO_3$-*m*	3.68	Indirect	1.45	
$ZnSiO_3$-*r*	4.18	Indirect	2.80	
Zn_2SiO_4-*t*	2.22	Direct	2.45	
Zn_2SiO_4-*r*	2.83	Direct	1.44	5.50,[a] 5.30,[b] 6.15,[c] 6.26,[d]
Zn_2SiO_4-*c*	2.78	Direct	2.11	4.36[e]

[a]Sol-gel derived zinc silicate phosphor films used for full-color display applications (Ref. 10).
[b]ZnO nanoparticles formed in SiO_2 by ion implantation combined with thermal oxidation (Ref. 43).
[c]ZnO particles embedded into SiO_2 by reactive magnetron sputtering (Ref. 19).
[d]ZnO particles embedded into SiO_2 by reactive magnetron sputtering (Ref. 19).
[e]Zn_2SiO_4 formed at the Si-ZnO interface (Ref. 17).

The ability to easily conduct electricity is one of the key feature of TCOs. Qualitative information about this feature can be derived from the analysis of the band dispersion at the band extremes. Analysis of Fig. 2 shows that the bottommost CB for all polymorphs of $ZnSiO_3$ and Zn_2SiO_4 are well dispersive. Consequently, one can expect that the electrical conductivity by CB electrons is favorable in these materials and this can be achieved by electron doping. Compared with the bottommost CB, the topmost VB for $ZnSiO_3$ and Zn_2SiO_4 phases are almost dispersionless in the whole Brillouin zone. So, electrical conductivity by holes cannot be as good as that by CB electrons. This behavior also indicates that the outermost valence electrons are tightly bonded to their host atoms. As discussed in Sec. III B, strong contribution to the topmost VB is coming from O and Zn atoms whereas that from Si is negligible. Consequently, one can suggest that the outermost VB electrons are tightly bonded to O and the Zn–O bond has a distinct ionic component. The dispersive nature of the topmost VB is largest for the $ZnSiO_3$-*r*, Zn_2SiO_4-*t*, and Zn_2SiO_4-*c* polymorphs. This indicates that different hybridization schemes play an important role for the carrier mobility.

B. Density of states

The band structure in the vicinity of CB and VB edges are analyzed above. Knowledge on the distribution of all valence electrons is obtained from the density of states (DOS). Such analyses are performed for the zinc silicate polymorphs in Fig. 3. It is seen that the VB consists of two major regions. The lower VB1 region in the energy range from −20 to −17 eV is relatively narrow and splits into sharp subbands. The VB2 region above VB1 covers the range from −9.5 to VB maximum and has broad features. In order to gain more insight into the VBs and CBs as well as into the chemical bonding, the orbital and site projected DOS

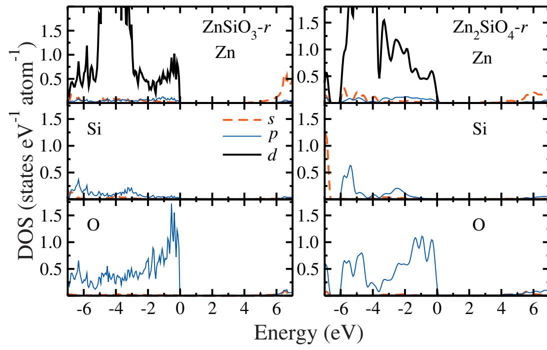

FIG. 4. (Color) The orbital and site-projected DOS for monoclinic $ZnSiO_3$-*m*, and Zn_2SiO_4-*r*. The Fermi level is set to zero.

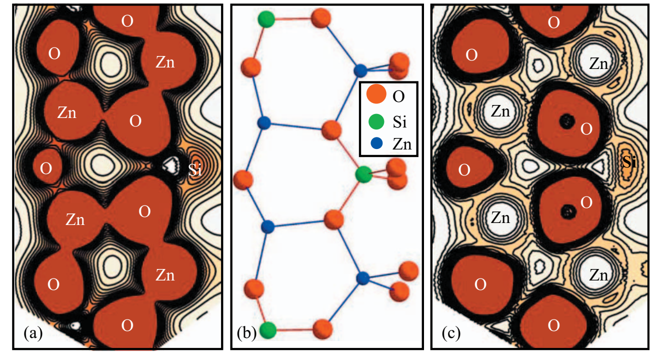

FIG. 5. (Color) (a) Charge density and (c) ELF for Zn_2SiO_4-*r* corresponding to the atomic plane schematically presented in (b).

(PDOS) were analyzed. Figure 4 shows the PDOS for $ZnSiO_3$-*m* and Zn_2SiO_4-*r*. It is seen that VB1 consists mainly of O 2*s* with smaller contributions from hybridized Si 3*s* and 3*p* electrons. The VB2 consists of three parts: The lowest energy region is basically contributed from Si 3*s* electrons. The intermediate energy region consists of very sharp peaks located around −5 eV that originates from Zn 3*d* electrons. The topmost part is hybridized Zn 3*d* and the O 2*p* states, while contributions from Si 3*p* states are negligible. This indicates that the topmost VB can drastically be modified by controlling the Zn and/or O stoichiometry.

The CB edge is well dispersed and consists basically of Zn 4*s* electrons, with smaller contribution from both O 2*s* and Si 3*s*. Hence, the Zn 4*s* electrons at the CB minimum play an important role in the electrical conductivity for all these zinc silicate polymorphs. Since the contribution from the Si 3*s* and O 2*s* electrons to the CB edge is smaller than that from the Zn 4*s* electrons, one can say that they play almost no role in the effective mass of the CB electrons.

The large band gap means that the band offset between the zinc silicate and Si or ZnO will be large. The offset between CBs and VBs of *n*-ZnO and p^+-Si is 0.30 eV (Ref. 32) and 2.55 eV,[33] respectively. Since the band gap of $ZnSiO_3$ and Zn_2SiO_4 polymorphs can be larger than that of ZnO, one can expect that the offset between CB(VB)s of the silicates and ZnO(Si) will be different from the above mentioned values. This will certainly affect the performance of device structures.

C. CB effective masses

As noted above (see also Fig. 2), the states at the CB minimum are much more dispersive than the topmost VB states. Consequently, CB electrons are lighter than holes and hence the influence of the latter on the electrical conductivity will be minimal. For quantitative characterization of carrier mobility, the calculated effective masses around the bottommost CB extremes are given in Table II. Analysis shows that the effective masses for electrons in $ZnSiO_3$ and Zn_2SiO_4 polymorphs are almost isotropic. Hence, the CB electron mobility and electrical conductivity of the compounds are expected to be isotropic as well. At present there are no experimental data available.

The CB electron masses for $ZnSiO_3$-*o*, $ZnSiO_3$-*m* and Zn_2SiO_4-*t* are of the same magnitude, whereas those for Zn_2SiO_4-*r* are about four times larger. Hence, the electrical conductivity for Zn_2SiO_4-*r* is expected to be smaller than that for other modifications of $ZnSiO_3$ and Zn_2SiO_4. The calculated CB electron effective mass of around $1.24m_0$ for Zn_2SiO_4-*r* is, however, much larger than that for well known TCOs, for example, $0.23m_0$ (Ref. 34) and $0.24m_0$ (Ref. 35) for ZnO, $\sim 0.23m_0$ for Zn_2SnO_4, $\sim 0.18m_0$ for Cd_2SnO_4, and $\sim 0.17m_0$ for $CdIn_2O_4$.[24] Consequently, the mobility of CB electrons as well the electrical conductivity in Zn_2SiO_4-*r* is expected to be small.

D. Chemical bonding and charge density analysis

A more detailed understanding of the bonding behavior can be obtained from charge density and electron localization function (ELF) analysis.[36–38] Figure 5(a) presents the charge density distribution for Zn–O and Si–O bonds of Zn_2SiO_4-*r*. The compounds Zn_2SiO_4-*t*, $ZnSiO_3$-*o*, $ZnSiO_3$-*m*, and $ZnSiO_3$-*r* exhibit similar features to that of Zn_2SiO_4-*r*. It is found that the largest charge density is residing at the Zn and O atoms. A large amount of localized electrons are present around Zn. These are semicore Zn 3*d* electrons considered as valence electrons in the computation. The charge around Si

TABLE II. Effective masses of CB electrons (in units of free-electron mass m_0) for $ZnSiO_3$ and Zn_2SiO_4 polymorphs along with those for ZnO.

$ZnSiO_3$-*o*	$ZnSiO_3$-*m*	Zn_2SiO_4-*r*	Zn_2SiO_4-*t*	ZnO
0.372($\Gamma \to$X)	0.335($\Gamma \to$A)	1.226($\Gamma \to$F)	0.316($\Gamma \to$N)	0.14,[a] 0.23,[b] 0.24[c] ($\Gamma \to$A)
0.353($\Gamma \to$W)	0.430($\Gamma \to$Z)	1.240($\Gamma \to$L)	0.378($\Gamma \to$X)	0.14,[a] 0.21[b] ($\Gamma \to$M)
0.390($\Gamma \to$Y)		1.240($\Gamma \to$Z)	0.470($\Gamma \to$Z)	

[a]Calculated by VASP (Ref. 44).
[b]Calculated from full-potential linear muffin-tin orbital method (Ref. 34).
[c]Experimental value from Ref. 35.

is smaller than that around Zn. On the one hand, this is because Si does not have *d* electrons and, on the other hand, as demonstrated by the analysis of the Bader charge in the following section, Si donates to O more charge than Zn. This result is consistent with the analysis of PDOS (Fig. 4), which shows that the population of the Si site by electrons is smaller than that of the Zn. This result is reasonable also because the spectroscopic electronegativities of Zn and Si are 1.65 and 1.90,[39] respectively. Since the electronegativity of O is 3.44, the ionic interaction between Zn and O as well as between Si and O is more enhanced than covalent bonding.

According to PDOS (Fig. 4), the bonding mechanism in the zinc silicates is the hybridization between Zn 3*d*, Si 3*p*, and O 2*p* states. The Si–O bonds can be characterized as having both ionic and covalent characters: covalent because the O 2*p* states are noticeably hybridized with Si 3*p* states in large energy range in close vicinity of the CB and VB edges, ionic because the main peaks of O 2*p*, Zn 4*s*, and Si 3*p* states are located in different energy ranges. Contribution of the O 2*p* states is predominant in the energy range −1 to 0 eV, whereas the Zn 4*s* and Si 3*p* states are dominant in the bands located in close vicinity of the CB edge.

The ELF is a useful tool to characterize the chemical bonding[40–42] as it measures the probability distribution of paired electrons. Figure 5(b) presents the calculated ELF plot. Analysis shows that the ELF value is small around Zn and Si. The ELF distribution around O is larger and this shows that the electrons are transferred from Zn and Si to the O sites, i.e., strong ionic character. The ELF contours are not spherically shaped indicating the presence of noticeable directional bonding.

The smallest and largest distances between Zn and O atoms in the zinc silicates in Fig. 5 are 1.972 and 1.952 Å, respectively. Those between Si and O are equal to 1.637 and 1.611 Å. This result indicates that the strongest bonding in this solid is between Si and O, which might possess covalent character as well. It follows from analysis of Fig. 4 that in the energy range −4 to 0 eV where the O 2*p* have the strong weight, there are also Si 3*s* and 3*p* as well as Zn 4*p*-like electrons, and 3*d* and 4*s* electrons. As discussed in previous studies,[30] this result indicates to the existence of covalence in the chemical bonding between Si and O as well as between Zn and O. Furthermore, the nonspherical charges around the Zn, Si, and O atoms are the indications of the covalent character of the chemical bonding. covalence.

For quantitative analysis of charge transfer, several schemes are available for partitioning the space between atoms. In this work, we use Bader and Voronoi charge analysis.[36–38] According to the Bader topological analysis, each atom is surrounded by a surface that run through minima of the charge density. These regions are known as Bader regions. This partitioning estimates the total charge around each atom by integrating the electron density within the Bader region. In the Voronoi charge analysis, each grid point of charge density is assigned to the nearest atom, but these distances are not scaled by the radius of the involved atom. The reported Voronoi charges are presently just used for checking of consistency.

TABLE III. Atomic effective charges (in units of electron charge e^-) within the atomic basins of Zn, Si, and O calculated according to Bader's topological analysis (denoted by Bader) and Voronoi deformation density (denoted by Voronoi) in $ZnSiO_3$-*m*, Zn_2SiO_4-*r*, Zn_2SiO_4-*t*, and ZnO.

Compound	Atom	Voronoi	Bader
$ZnSiO_3$-*m*	Zn	0.91	0.65
	Si	1.41	2.00
	O1	−0.69	−0.81
	O2	−0.71	−0.78
	O	−0.78	−1.06
Zn_2SiO_4-*r*	Zn1	0.38	0.65
	Zn2	0.88	0.68
	Si	1.52	1.89
	O1	−0.87	−0.85
	O2	−0.88	−0.87
	O3	−0.81	−0.76
	O4	−0.49	−0.74
Zn_2SiO_4-*t*	Zn1	0.78	0.60
	Zn2	0.85	0.61
	Si	1.45	1.96
	O1	−0.91	−0.82
	O2	−0.46	−0.72
	O3	−0.77	−0.79
	O4	−0.90	−0.84
ZnO	Zn	0.26	0.55
	O	−0.70	−0.55

The results for some zinc silicates are presented in Table III. As expected, Zn and Si atoms donate electrons, while O atoms are acceptors. The amount of the donated charge indicates ionic type of chemical bonding between Zn and O as well as polar covalent bonding between Si and O. Analysis shows that the amount of charge donated by Zn to O in the zinc silicates is larger than that in ZnO.

E. Optical properties

Figure 6 presents the optical dielectric response function for $ZnSiO_3$ and Zn_2SiO_4. In order to describe the optical anisotropy, three diagonal components of the dielectric func-

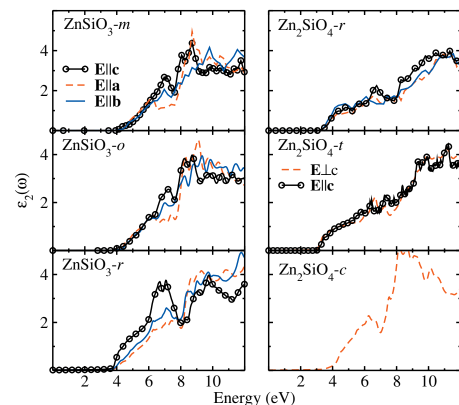

FIG. 6. (Color) Dielectric response functions for polymorphs of $ZnSiO_3$ and Zn_2SiO_4 for the different directions of the electric field **E** compared to the **a**, **b**, and **c** axes.

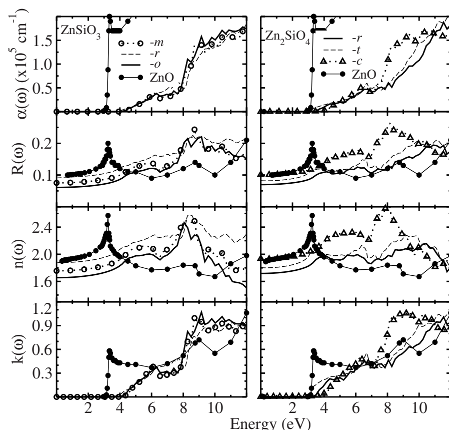

FIG. 7. (Color online) The calculated optical spectra for $ZnSiO_3$ and Zn_2SiO_4 polymorphs as compared to those determined experimentally for ZnO (Ref. 45).

tion are calculated for $ZnSiO_3$-*o*, six for $ZnSiO_3$-*m*, and two for Zn_2SiO_4-*t* and Zn_2SiO_4-*r*. Among the six components for $ZnSiO_3$-*m*, the off-diagonal components are found to be negligible and hence the analysis is made just for the three diagonal components corresponding to the electric field **E** parallel to the crystallographic **a**, **b**, and **c** axes. Cubic Zn_2SiO_4-*c* has isotropic optical properties.

Figure 6 presents the imaginary part of the optical dielectric function as a function of energy $[\varepsilon_2(\omega)]$ with electric field along different optical directions. The variation in $\varepsilon_2(\omega)$ for different crystallographic directions is very small. Consequently, the optical spectra are more or less isotropic. Figure 7 displays the absorption coefficient $\alpha(\omega)$, reflectivity $R(\omega)$, refractive index $n(\omega)$, and extinction coefficient $k(\omega)$ for polymorphs of $ZnSiO_3$ and Zn_2SiO_4. The analyses of Figs. 6 and 7 show that the optical spectra are quite independent of crystallographic direction and lattice type. Consequently, amorphous $ZnSiO_3$ and Zn_2SiO_4 might possess similar optical properties as their crystalline counterparts at energies larger than the fundamental band gap.

Analysis of Fig. 7 shows that in the energy range 0–4 eV, the calculated absorption coefficient $\alpha(\omega)$, reflectivity $R(\omega)$, refractive index $n(\omega)$, and extinction coefficient $k(\omega)$ for zinc silicates are considerably smaller than those determined experimentally for ZnO. It is well known that DFT underestimates the band gaps. Consequently, the calculated optical spectra will be shifted toward lower energies relative to the experimental spectra. To fix error, sometimes the optical spectra are rigidly shifted toward larger energies up to the experimentally determined location. Since no experimental data are available in the present work, the rigid shift technique has not been applied. Hence, one can expect that $\alpha(\omega)$, $R(\omega)$, $n(\omega)$, and $k(\omega)$ of the $ZnSiO_3$ and Zn_2SiO_4 polymorphs will be smaller than those of ZnO in wider energy range than 0–4 eV (Fig. 7). Currently, the theoretical results indicate the possibility of using these silicates as antireflection coatings. Studies of defects, electrical current transport properties of the zinc silicates and their band alignment with other semiconductors will be the subject of future studies. We hope that our theoretical results will motivate experimental studies on these materials.

IV. CONCLUSIONS

The presents *ab initio* studies of electronic structure and optical properties of $ZnSiO_3$ and Zn_2SiO_4 polymorphs show that these compounds are wide band gap solids with direct or indirect band gap depending on type polymorph. The bottommost CB is dispersive and is contributed mainly by Zn 4*s* electrons. The topmost VB is almost dispersionless and is contributed by O 2*p* and Zn 3*d* electrons. From considerations of charge density, Bader and Voronoi charge calculations, and ELF, it is shown that these compounds possess significant ionic contributions to the bonding. The optical properties of all compounds are close to isotropic and for these the particular structural modification appears to have less importance. Based on the magnitude of the absorption coefficient ($<10^3$ cm^{-1}), reflectivity (<0.15), refractive index (<2.20), and extinction coefficient (<0.30), all these $ZnSiO_3$ and Zn_2SiO_4 polymorphs can be used as antireflection coatings in optoelectronic devices.

ACKNOWLEDGMENTS

This work has been funded by the Research Council of Norway through the NANOMAT program and from FOET Project No. 142327. Supercomputing support has been received from NOTUR facilities. S.Z.K thanks Dr. A. Klaveness and Dr. K. Knizek (Institute of Physics ASCR, Prague, Czech Republic) for discussions and help in computations.

[1]J. M. Keijman, *PCE '99 Conference* (The Brighton Centre, Brighton, England, 1999).
[2]P. Tao, M. Mei-Hua, X. Fei-Bo, and X. Xin-Quan, Appl. Surf. Sci. **181**, 191 (2001).
[3]N. Taghavinia, H. Y. Lee, H. Makino, and T. Yao, Nanotechnology **16**, 944 (2005).
[4]J. M. Yuk, J. Y. Lee, Y. S. No, T. W. Kim, and W. K. Choi, Appl. Phys. Lett. **93**, 221910 (2008).
[5]J. W. Shin, Y. S. No, T. W. Kim, and W. K. Choi, J. Nanosci. Nanotechnol. **8**, 5566 (2008).
[6]J. M. Yuk, J. Y. Lee, J. H. Jung, D. U. Lee, T. W. Kim, D. I. Son, and W. K. Choi, J. Appl. Phys. **103**, 083520 (2008).
[7]G. T. Chandrappa, S. Ghosh, and K. C. Patil, J. Mater. Synth. Process. **7**, 273 (1999).
[8]K. C. Mishra, K. H. Johnson, B. G. Deboer, J. K. Berkowitz, J. Olsen, and E. A. Dale, J. Lumin. **47**, 197 (1991).
[9]M. Cich, K. Kim, H. Choi, and S. T. Hwang, Appl. Phys. Lett. **73**, 2116 (1998).
[10]Q. Y. Zhang, K. Pita, and C. H. Kam, J. Phys. Chem. Solids **64**, 333 (2003).
[11]B. W. Jeoung, G. Y. Hong, B. Y. Han, and J. S. Yoo, Jpn. J. Appl. Phys. **43**, 7997 (2004).
[12]J. Wan, X. Chen, Z. Wang, L. Mu, and Y. Qian, J. Cryst. Growth **280**, 239 (2005).
[13]F. H. Su, B. S. Ma, K. Ding, G. H. Li, S. P. Wang, W. Chen, A. G. Joly, and D. E. McCready, J. Lumin. **116**, 117 (2006).
[14]I. Kandarakis, D. Cavouras, P. Prassopoulos, E. Kanellopoulos, C. D. Nomicos, and G. S. Panayiotakis, Appl. Phys. A: Mater. Sci. Process. **67**, 521 (1998).
[15]X. Xu, P. Wang, Z. Qi, M. Hai, J. Xu, H. Liu, C. Shi, G. Lu, and W. Ge, J. Phys.: Condens. Matter **15**, L607 (2003).
[16]X. L. Xu, C. X. Guo, Z. M. Qi, H. T. Liu, J. Xu, C. S. Shi, C. Chong, W. H. Huang, Y. J. Zhou, and C. M. Xu, Chem. Phys. Lett. **364**, 57 (2002).
[17]U. Meier and C. Pettenkofer, Appl. Surf. Sci. **252**, 1139 (2005).
[18]O. Kluth, B. Rech, L. Houben, S. Wieder, G. Schope, C. Beneking, H. Wagner, A. Loffl, and H. W. Schock, Thin Solid Films **351**, 247 (1999).
[19]J. G. Ma, Y. C. Liu, C. S. Xu, Y. X. Liu, C. L. Shao, H. Y. Xu, J. Y. Zhang, Y. M. Lu, D. Z. Shen, and X. W. Fan, J. Appl. Phys. **97**, 103509 (2005).
[20]H. Chang, H. D. Park, K. S. Sohn, and J. D. Lee, J. Korean Phys. Soc. **34**,

545 (1999).
[21]H. Zhang, X. Feng, and J.-Y. Kang, Chin. J. Lumin. **27**, 68 (2007).
[22]G. Kresse and J. Furthmüller, Phys. Rev. B **54**, 11169 (1996).
[23]X. Jiang and G. Y. Guo, Phys. Rev. B **69**, 155108 (2004).
[24]D. Segev and S. H. Wei, Phys. Rev. B **71**, 125129 (2005).
[25]S. Z. Karazhanov, P. Ravindran, P. Vajeeston, A. Ulyashin, H. Fjellvag, and B. G. Svensson, J. Phys.: Condens. Matter **21**, 485801 (2009).
[26]J. P. Perdew and A. Zunger, Phys. Rev. B **23**, 5048 (1981).
[27]D. M. Ceperley and B. J. Alder, Phys. Rev. Lett. **45**, 566 (1980).
[28]P. E. Blöchl, Phys. Rev. B **50**, 17953 (1994).
[29]G. Kresse and D. Joubert, Phys. Rev. B **59**, 1758 (1999).
[30]P. Ravindran, A. Delin, R. Ahuja, B. Johansson, S. Auluck, J. Wills, and O. Eriksson, Phys. Rev. B **56**, 6851 (1997).
[31]S. Z. Karazhanov, P. Ravindran, A. Kjekshus, H. Fjellvag, and B. G. Svensson, Phys. Rev. B **75**, 155104 (2007).
[32]K. B. Sundaram and A. Khan, J. Vac. Sci. Technol. A **15**, 428 (1997).
[33]X. Li, B. Zhang, X. Dong, Y. Zhang, X. Xia, W. Zhao, and G. Du, J. Lumin. **129**, 86 (2009).
[34]W. R. L. Lambrecht, A. V. Rodina, S. Limpijumnong, B. Segall, and B. K. Meyer, Phys. Rev. B **65**, 075207 (2002).
[35]K. Hümmer, Phys. Status Solidi B **56**, 249 (1973).
[36]G. Henkelman, A. Arnaldsson, and H. Jonsson, Comput. Mater. Sci. **36**, 354 (2006).
[37]C. Fonseca Guerra, J.-W. Handgraaf, E. J. Baerends, and F. M. Bickelhaupt, J. Comput. Chem. **25**, 189 (2004).
[38]R. F. W. Bader, *Atoms in Molecules: A Quantum Theory* (Oxford University Press, New York, 1990).
[39]A. L. Allred, J. Inorg. Nucl. Chem. **17**, 215 (1961).
[40]A. D. Becke and K. E. Edgecombe, J. Chem. Phys. **92**, 5397 (1990).
[41]B. Silvi and A. Savin, Nature (London) **371**, 683 (1994).
[42]P. Vajeeston, P. Ravindran, R. Vidya, A. Kjekshus, and H. Fjellvag, Europhys. Lett. **72**, 569 (2005).
[43]H. Amekura, K. Kono, N. Kishimoto, and C. Buchal, Nucl. Instrum. Methods Phys. Res. B **242**, 96 (2006).
[44]S. Z. Karazhanov, P. Ravindran, A. Kjekshus, H. Fjellvag, U. Grossner, and B. G. Svensson, J. Appl. Phys. **100**, 043709 (2006).
[45]S. Adachi, *Optical Constants of Crystalline and Amorphous Semiconductors. Numerical Data and Graphical Information* (Kluwer Academic Publishers, Boston, Dordrecht, London, 1999).